NUMERICAL ANALYSIS OF THE METHOD OF INTERNAL DIALYSIS OF GIANT AXONS

LYLE W. HORN
Department of Physiology/Biophysics, Temple University Health Sciences Center, Philadelphia, Pennsylvania 19140

ABSTRACT This paper presents a numerical analysis of the method of internal dialysis used for studies of membrane transport in giant axons. Account is taken of the complete geometry, end effects, and finite dialyzate flow rates. Both influx and efflux experimental conditions are considered. Results place quantitative limits on system performance that are sufficiently general for use in experimental design. The completeness of solute equilibration and the uniformity of solute concentration at the axon membrane are assessed, as well as the sensitivity to dialysis solution flow rate. The effects of undialyzed axon ends on the equilibration rate and on the uniformity of concentration are determined, and the contribution of undialyzed ends to influx measurements is evaluated. Equilibration times are correlated with physical properties of axoplasm and dialysis tubing, and with dialysis solution flow rate. Numerical results confirm the general qualitative assessments of the method that are based on years of successful application.

INTRODUCTION

Since Brinley and Mullins (1967) introduced the technique of internal dialysis for the control of intracellular solute compositions in squid giant axons, the method has become a standard for membrane transport studies in giant nerve and barnacle muscle fibers. The method involves inserting a small capillary tube along the axis of the axon and out the other end. The tube is permeable to water and low molecular weight solutes only over ~1 cm of its length. Solutions of permeable solutes flowing through the tubing should, in principle, equilibrate with the axoplasm and establish a known intracellular composition in the dialyzed region. The efflux of a solute can be measured by placing a radioactive tracer in the dialysis solution and collecting the tracer that appears in the external solution. The influx of a solute can be measured by bathing the cell in radioactive solution and collecting the tracer that appears in the internal dialysis solution.

Years of experience with this technique have shown that it works fairly well, especially for efflux measurements. However, certain questions arise that are important at least for the design of protocols, and whose answers would enhance the degree of confidence in results obtained by the method. The first question is how closely the solute concentration at the cell membrane approaches that in dialysis solution in the dialyzed region of the cell in the steady state. We need to know how uniform the concentration is along the length of dialyzed region and how sensitive the axial solute field is to the dialysis solution flow rate. The influence of the undialyzed ends of the cell on the solute field in the dialyzed region is also unknown. Estimates of the time required to reach a steady state in the dialyzed region would be very useful, as would estimates of the rate of development of the end effects.

These questions cannot be answered solely by experiment because the measurements required are not practical. A theoretical analysis of the system is required that can place reasonable limits on the performance demanded of the method. Brinley and Mullins (1967) performed a cursory analysis that was restricted to infinite dialyzate flow rate, one axoplasm diffusivity and one tubing permeability, and allowed only radial diffusion. They were unable to analyze end effects satisfactorily. It is the purpose of this communication to present a more general analysis of the system that takes account of the three-dimensional geometry, the end effects, and finite dialyzate flow rates.

THEORY

Fig. 1 defines the geometry of the system and relevant symbols. It is assumed that no chemical reactions occur, that the flow of fluid in the dialysis tube is laminar, that there is no bulk flow of water radially through the permeable wall of tubing, that the concentration of solute in dialysis solution is uniform and constant at the point where flowing fluid enters the permeable wall region, and that the extreme ends of the axon are impermeable.

The laminar flow assumption is valid because Reynolds numbers for typical tubing diameters and solution flow rates are <10. Brinley and Mullins (1967) concluded that water filtration is $<2\%$ of the axon volume per hour so that radial bulk solvent flow should be very small. Within the lumen of the permeable region of the dialysis tube, radial diffusion relaxation times can be of about the same order as axial mean transit times through the porous region. Therefore radial diffusion cannot be ignored in the dialysis solution. This fact requires that the true parabolic velocity profile be taken into account. Axial diffusion must be considered not only in the cell but also in dialysis fluid. The Peclet number for typical operating conditions can be $<<$ 100, so that axial diffusion could be

significant at least near the ends of the permeable region where $\partial^2 C/\partial x^2$ could be large.

The general diffusion equation for this system is

$$\partial C/\partial t + U[1 - (r/r_i)^2]\partial C/\partial x = D[\partial^2 C/\partial x^2 + (1/r)\partial C/\partial r + \partial^2 C/\partial r^2] \quad (1)$$

where C = solute concentration; t = time; x = axial distance; r = radial distance; r_i = dialysis tube inner radius; U = maximum dialysis fluid velocity; $U = 0$ for $r \geq r_i$; D = solute diffusion coefficient; $D_t = D$ in dialysis solution; $D_w = D$ in tubing wall; $D_a = D$ in axoplasm. There are six regions in this system: the dialysis solution in the lumen of the porous tubing wall zone, dialysis solution in the tubing lumen downstream of the porous wall zone, the porous tubing wall, the axoplasm in the porous wall zone, and the undialyzed axoplasm above and below the porous wall zone (Fig. 1).

Boundary conditions for adjoining regions require equality of concentration and flux. The flux normal to the surface must be zero at the surfaces of the nonporous tubing, and all gradients must be zero in the dialysis solution in the tubing lumen infinitely far downstream of the porous region. At the axon membrane a simple permeability boundary condition is utilized:

$$D_a[\partial C/\partial r] = P(C_o - C), \qquad r = r_a \quad (2)$$

where P is the cell membrane permeability to solute and C_o is the extracellular solute concentration. C_o is assumed constant in time but may vary with axial distance.

Each of the six regions of this system is governed by its own geometric and time scales. It is not possible to characterize the performance of the system by means of only one or two parameters. When the equations for each region are scaled geometrically and temporally, eight independent, dimensionless groups are obtained that uniquely determine the solution of the system of equations for any set of initial conditions. The groups are important because the solution to the equations is independent of the magnitudes of the individual parameters that form them. These groups comprise a set of similarity parameters that completely specify the system. Any real system with similarity parameters equal to those utilized in this work will have the same scaled theoretical behavior as presented herein, no matter what the absolute values of individual geometric or physical quantities may be.

There are four geometric and four dynamic similarity parameters, given below:

Geometric

$$l_t/r_i \quad (3a)$$

$$r_i/r_o \quad (3b)$$

$$l_t/(r_a - r_o) \quad (3c)$$

$$l_a/l_t \quad (3d)$$

Dynamic

$$D_t/(Ur_i) \quad (4a)$$

$$D_w/D_t \quad (4b)$$

$$D_a/D_w \quad (4c)$$

$$P(r_a - r_o)/D_a. \quad (4d)$$

A comprehensive study of the solutions to the system Eq. 1 would require that the role of each similarity parameter be evaluated. However, in actual experimental practice the most variable quantities are r_a, P, D_a, and U. Similarity parameters (Eqs. 3c, 4a, and 4c) are of greatest interest. Parameter 4d is not as important because its magnitude is very much less than 1 for most solutes. Eq. 4d does assume some importance when isotope influx conditions are considered, however.

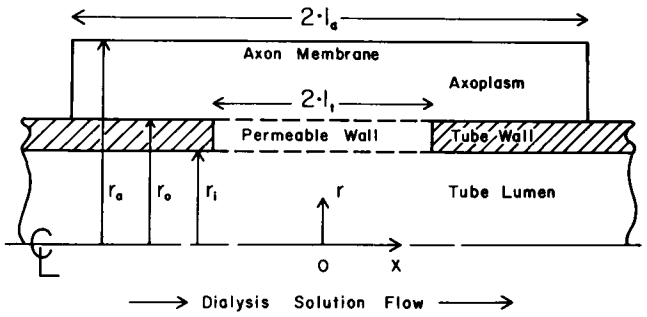

FIGURE 1 Geometry of the dialyzed axon system showing one-half of an axial cross section through concentric cylinders. r_a is axon radius, r_o is tubing outside radius, r_i is tubing internal radius, l_a is axon half-length and l_t is half-length of permeable tubing wall. Note location of coordinate axes on system center line.

The axoplasm aspect ratio, Eq. 3c, is a comparison of the total surface area for radial diffusion in the dialyzed region to that for axial diffusion between dialyzed and undialyzed regions of the axon. It is relevant to an evaluation of end effects on dialysis efficiency. Parameter 4a is a measure of the efficiency of solute delivery to the permeable dialysis membrane by dialysis solution flow. Parameter 4c should determine whether axoplasm or tubing wall diffusion controls the rate of equilibration of axoplasm with dialysis solution. The tubing wall porosity, Eq. 4b, is important, of course, but is likely to be relatively independent of the solute type for the most commonly used solutes of low molecular weight (Farrell and Babb, 1973). Parameter 4d is a comparison of the rate of cell-membrane solute flow to solute diffusion in axoplasm.

Because the geometry and boundary conditions for this system are quite complicated, an analytical solution of Eq. 1 is not possible. A numerical integration is required.

Numerical Analysis

Numerical integration of Eq. 1 is very difficult because the geometry is two-dimensional and complex, there are six independent spatial regions, and diverse length and time scales for each region can lead to stiff equations. Extremely large computer memory and time would be required if standard finite difference methods were used. I have sought to make the problem tractable by means of a finite element method (Villadsen and Sorensen, 1969; Villadsen and Stewart, 1967) coupled with an implicit multistep integration in the time domain, which is designed for stiff systems (Gear, 1971). Detailed information about the structure of the solute concentration field in each region of the system is lost by this approach. However, information about the field near the system boundaries and about the development of the field in time is obtained and should permit a fairly general characterization of the system for usual laboratory operating conditions.

Each of the six spatial regions is mapped onto a square of unit dimensions. The infinite region of dialysis solution downstream of the permeable wall zone is approximated by an axial distance of at least 100 dialysis tubing diameters and then mapped. Within each region the concentration field is approximated by a series expansion in N axial and M radial orthogonal polynomials. The residual error of the differential equation due to the approximation is also an orthogonal polynomial, and can be made identically zero by applying the field approximation only at the true zeroes of the residual polynomial (Villadsen and Stewart, 1967). A two-dimensional finite element grid is thus established, each point defined by one axial, radial zero pair, which covers each spatial region with $N \times M$ points. Practically, N and M need be no larger than 4. Lagrangian interpolation formulas for the spatial operators of the differential equations are then derived utilizing these zero points. One obtains a

set of first-order ordinary differential equations in the time domain, which can be integrated for any set of initial conditions. The final form of the differential equations in each region is

$$\mathbf{dC}/dt = \mathbf{A} \cdot \mathbf{C}$$

where **A** is the two-dimensional matrix of Langrangian interpolation coefficients for the axial and radial spatial operators and **C** is the two-dimensional matrix of concentrations that define the field at the axial and radial polynomial zeroes within each region.

Boundary concentrations are included in the matrix **C** even though the boundary points are not zeroes of orthogonal polynomials. Thus, the residuals of the differential equations will not be identically zero. It is postulated that the residuals are small. The validity of the approximation is checked by integrating the equations for a system with a known analytic solution. The cell membrane boundary condition is incorporated directly into the differential equations. All other boundary concentrations are calculated explicitly from the boundary conditions by means of standard finite difference formulas.

Chebychev polynomials have proved very useful for numerical approximations of complicated functions and solutions of differential equations (Lanczos, 1956). They are particularly useful for the present problem because their zeroes are weighted toward the system boundaries, and the boundaries are of primary interest in this work. Although any orthogonal polynomial might be used in principle, in practice not all will work. Trial and error testing by means of analytic solutions is required to establish the reliability of a polynomial. I have tested Chebychev, Legendre, and Jacobi polynomials and found that Chebychevs consistently give the best results (Table I).

Concentrations were normalized to fall in the range of 0 to 1, to maintain consistent computational accuracy among many possible operating conditions. The normalizing concentration, C^*, was defined as

$$C^* = \text{Max}\ (C_i, C_u, C_o)$$

where

C_i = initial concentration in axoplasm, assumed uniform

C_u = concentration in dialysis solution upstream from the permeable wall

and

C_o = extracellular concentration.

Computations were done on a Univac 1108 using double precision (64 bit word) or on a Cyber 174 using single precision (60 bit word) arithmetic. This degree of precision was essential for reliable results due to the stiffness of the equations.

It should be noted that if four radial and four axial grid points are used in each region, 108 differential equations must be integrated in the time domain. Because the equation system can be very stiff, many hours of computer time could be required to integrate only part of the way to steady state. Thus, in many cases accuracy was sacrificed in favor of speed by reducing the number of grid points in some regions. The radial grid was always comprised of four points in axoplasm and two each in the wall and tubing lumen, for a total of eight points in the central zone. The axial grid consisted of three or four points in the central zone, two or four points in the undialyzed axon ends, and two points in the tubing lumen downstream from the permeable zone. Comparison of results using different numbers of axial grid points showed that the calculated concentration field in the central zone is not sensitive to the number of points but that in the undialyzed ends it is very sensitive. Thus, when end effects were considered, four axial grid points were usually used in each undialyzed end.

TABLE I
NUMERICAL ERRORS

Polynomial	No. grid points		
	4	6	8
Chebychev	20	12	7
Legendre	33	15	12
Jacobi ($\alpha = 1, \beta = 1$)	43	22	18
Jacobi ($\alpha = 2, \beta = 2$)	53	27	27

Effect of number of radial grid points (polynomial zeros) and type of polynomial on global error when diffusion is 98.5% complete. $K = 1$. Polynomials defined in Abramowitz and Stegun (1964). Error presented as percent of analytic solution values.

Program Test

The program was tested by comparing numerical integrations with a known analytic solution. The analytic problem is that of radial diffusion in an infinite cylinder with a permeability boundary condition at the cylinder surface. The analytic solution is given by Carslaw and Jaeger (1959, p. 202) as an infinite series of Bessel functions, which I evaluated for the first 20 terms. The initial condition was uniform concentration in the cylinder with zero concentration outside the cylinder. Although this test problem is a one-dimensional diffusion problem, it serves to test the scaling, the Lagrangian interpolation formulas for the spatial operators, the mapping of the spatial domains into unit squares, the boundary condition approximations, and the time domain integration. The axial Langrangian interpolation coefficients and axial boundary conditions were utilized in the computation as well, to detect errors from this source.

The analytic solution of the problem is characterized uniquely by one dimensionless parameter,

$$K = P \cdot r_a / D_a, \tag{5}$$

which is a measure of the rate of interfacial exchange relative to bulk diffusion. Solutions were obtained covering four orders of magnitude for K (10^{-2} to 10^{+2}). The value of the numerical solution was less than that of the analytic solution in all cases, but the numerically computed concentration field tended to be parallel to the true field at all times. Thus, the numerical computation gives an accurate representation of the spatial concentration distribution at any time, but tends to underestimate the time required to achieve a specified concentration. The inaccuracy of temporal estimates should not be serious, however, because it will be determined approximately by the natural logarithm of the error in the concentration estimate.

The global error is defined as the percent deviation of the numerical from the analytic solution. The largest global error occurred for the case of $K = 1$. The magnitude of the error was independent of the single step tolerance for integration in the time domain over the tolerance range 10^{-4} to 10^{-8}. Because the numerical and analytic solutions were approximately parallel, the global error increased with time as the concentrations approached zero. However, solutions remained approximately parallel up

TABLE II
COMMON PARAMETERS

r_a	250 μm	D_t	10^{-5} cm^2/s
r_o	70 μm	D_w	10^{-6} cm^2/s
r_i	47.5 μm	D_a	5×10^{-6} cm^2/s
l_t	0.5 cm	P	10^{-7} cm/s
l_a	1.5 cm	U	0.5 cm/s

List of most commonly used geometric and physical parameters. Geometric parameters defined in Fig. 1. Physical parameters defined in Eq. 1.

to 99.95% of completion, indicating the resolution of the numerical procedure is at least 1/1,000.

The global error was sensitive to the number of radial grid points and to the polynomial used to define the grid. Table I presents a comparison of global errors for the worst case of $K = 1$. It should be stressed that the numerical solution converges to the same final value (0, accurate to 10^{-4}) as the analytic, only faster. This is the principal source of error. Because the numerically determined concentration field parallels the analytic field, it was not deemed necessary to improve global accuracy.

An additional check for possible scaling errors was done by generating solutions for the worst case of $K = 1$, in which two of the three parameters defining K, Eq. 5, were changed by two orders of magnitude. Numerical solutions were identical among the three possible permutations of parameters.

The Chebychev polynomials are superior to the others in all cases. This is because their roots are clustered near the system boundaries. Therefore, all work on the dialysis problem was done utilizing Chebychev polynomials.

NUMERICAL RESULTS

An attempt was made to obtain numerical solutions of the dialysis system for parameter values in the range of those encountered experimentally (Table II). Deviations from these values are noted where appropriate. The time scale used in most cases is the radial diffusion relaxation time in axoplasm:

$$\tau_a = (r_a - r_o)^2/D_a. \quad (6)$$

However, for tracer influx computations, the time scale is defined in terms of the cell membrane permeability and surface-to-volume ratio

$$\tau = 0.5\,(r_a^2 - r_o^2)/(Pr_a). \quad (7)$$

The initial conditions used in most cases are of uniform, zero concentration in the cell, unit-normalized concentration in the dialysis solution, and constant zero external concentration. Because the cell membrane permeability is so small relative to bulk diffusion, the membrane is effectively impermeable, so that solutions for solute washout from the cell by dialysis can be obtained from the solute loading results simply by subtracting the normalized concentration from 1. Results can be applied either to considerations of control of cytoplasmic solute levels or to tracer efflux experiments in which only the tracer level changes with time. Tracer influx conditions are considered later.

A convenient measure of the solute distribution at the cell membrane is the total transmembrane flow, or the integral of the flux over the surface. This is the quantity actually measured experimentally. Because the flux across the membrane is given by a simple permeability relation, Eq. 2, the membrane flow is equivalent to a spatial mean concentration at the membrane, and the ratio of two membrane flows is exactly equal to the ratio of two mean concentrations at the membrane. The necessary integrals are evaluated from the calculated concentrations by numerical quadrature based on the appropriate grid points. Most results are presented in terms of total solute flows or flow ratios.

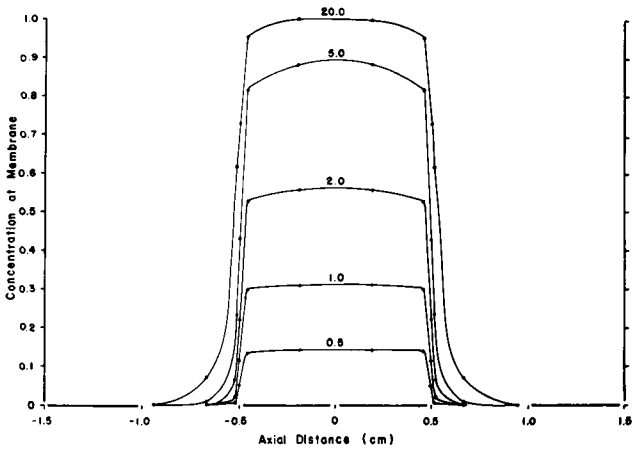

FIGURE 2 Development of axial solute concentration field at the cell membrane in 500 μm axon dialyzed at infinite flow. Parameters of Table II. Axial coordinates defined in Fig. 1. Dialyzed zone extends from − 0.5 to + 0.5 cm. Normalized concentration, C. $C = 1$ for all times in dialysis solution. $C = 0$ in axoplasm at time $t = 0$. Each curve is labeled with the scaled time elapsed from the start of dialysis. One time scale is 64.8 s, so that time for each curve can be read as approximate minutes. Points are computed values of C on the axial grid at $r = r_a$. Lines are drawn by eye to connect points smoothly, and may not be best interpolations between points.

Infinite Flow of Dialyzate

Efflux Conditions. Consider first the limiting case of an infinite dialysis solution flow rate. This case corresponds to a constant solute concentration at the inner surface of the dialysis tube equal to that in fresh dialysis solution, $C = 1$ at $r = r_i$ for all time. Fig. 2 shows the development of the solute concentration field at the cell membrane for the initial condition of no solute in the cell and the parameters given in Table II. The field representation is necessarily coarse because of the finite element method used. It is clear from Fig. 2 that the concentration at the membrane in the dialyzed zone is controlled effectively. Fig. 3 *A* shows the development of the cell membrane solute flow in the dialyzed region in time, while Fig. 3 *B* shows the development of the total cell membrane solute flow from the undialyzed ends of the axon. Axial diffusion into the undialyzed axon ends is significant, but it does not seriously distort the concentration field in the dialyzed region. Many hours of dialysis would be required before the solute efflux from the undialyzed ends reached the same magnitude as in the dialyzed zone.

Once the concentration in the dialyzed zone is essentially equal to that in dialysis solution, the solute will diffuse axially into the undialyzed ends roughly according to the relation for a semiinfinite solid (Carslaw and Jaeger, 1959, p. 60). In order that C in the undialyzed zone reach 90% of C in dialysis solution, 1 mm away from the boundary between dialyzed and undialyzed zones, it is necessary that

$$x^2/(4D_a t) \simeq 0.01$$

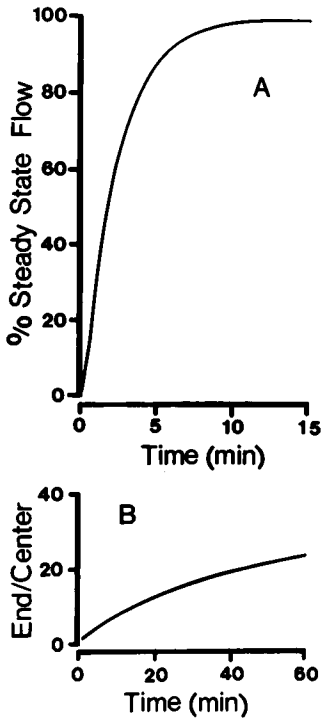

FIGURE 3 (*A*) Development of steady-state membrane flow in central dialyzed zone in time (min) for conditions of Table II. Curve can also be interpreted as the growth of the spatial mean solute concentration at the cell membrane in the dialyzed zone. (*B*) Development of end effect for same conditions as *A*. Ratio of total flow of solute across the undialyzed axon membrane to that in the central dialyzed zone (as percent) is plotted against time in minutes (note different time scales in *A* and *B*).

or

$$t \simeq 5 \times 10^4 \text{ s}.$$

This is double the typical duration of a complete dialysis experiment. Filling of the undialyzed ends by axial diffusion is extremely slow.

A negligible end effect cannot be expected for all experimental conditions, however. Table III demonstrates that the undialyzed ends of the cell have a negligible effect on the approach to a steady state in the central zone only if the aspect ratio, Eq. 3c, is greater than ~10. This general restriction corresponds to a total cross-sectional area for axial diffusion of <5% of that for radial diffusion in the central zone. The restriction should not be a practical problem with axons, but could pose difficulties for work with barnacle fibers whose diameters often exceed 1 mm. Other computations (not presented) show that the appoach to a steady state in the central zone is practically independent of the length of the undialyzed ends provided the aspect ratio is large. Of course, this is true only within the accuracy of the computations, which is much greater than experimental accuracy. It is concluded that for efflux conditions the response of the central zone to dialysis is independent of the undialyzed ends, provided the aspect ration is >10.

TABLE III
EFFECT OF ASPECT RATIO ON EQUILIBRATION

		Total solute flow across cell membrane (in percent)					
		500 μm Axon			800 μm Axon		
Scaled time	Dialyzed zone: 6 mm 10 mm 15 mm 3 mm 6 mm 10 mm Aspect ratio: 17 28 42 5 9 15						
0.00		0	0	0	0	0	0
0.25		5.0	4.9	4.8	4.3	5.8	5.9
0.50		15.3	15.2	15.0	12.3	16.7	17.2
1.0		33.4	33.2	32.4	25.0	35.0	36.3
2.0		59.0	58.9	58.6	42.3	59.2	62.1
5.0		91.1	91.3	91.1	63.7	87.5	92.0
10.0		100	100	100	71.3	96.2	97.4
15.0					73.3	97.1	99.8
20.0					74.3	97.5	100
60.0					76.7	100	

Effect of aspect ratio, Eq. 3c, on development of total solute flow across the cell membrane in central dialyzed zone for infinite dialysis solution flow rate. Parameters of Table II except that aspect ratio changed by varying either r_a or l_t. Normalized concentration $C = 1$ at $r = r_i$ for all times. $C = 0$ initially in axoplasm. Time scaled according to Eq. 6. One time scale is 64.8 s for 500 μm axon, and 218 s for 800 μm axon. Flow given as percent of ideal flow that would occur if $C = 1$ everywhere in axoplasm.

The critical quantity that determines the rate of approach to the steady state in the dialyzed zone is the ratio of radial diffusion time scales in the tubing wall and cytoplasm:

$$\tau_w/\tau_a = (D_a/D_w)[(r_o - r_i)/(r_a - r_o)]^2. \quad (8)$$

This time-scale ratio is obtained from the similarity parameters, Eqs. 3a–c, 4c. Therefore, regardless of the magnitudes of individual parameters that comprise it, a

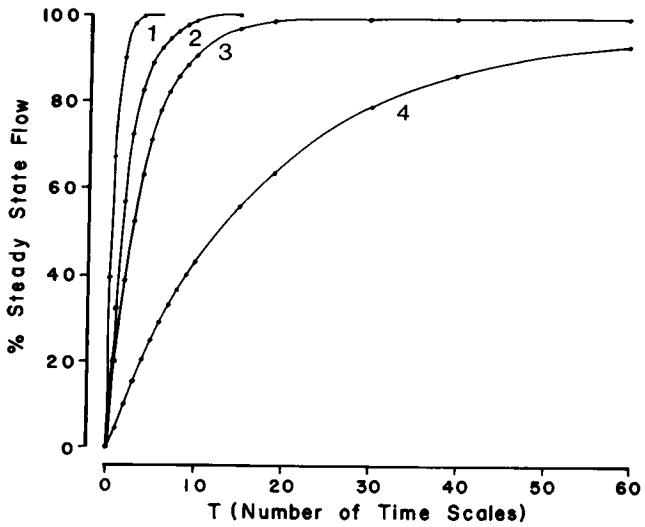

FIGURE 4 Solute equilibration at axon membrane in dialyzed zone at infinite dialysis solution flow. Curve *1*, $\tau_w/\tau_a = 0.008$; *2*, $\tau_w/\tau_a = 0.078$; *3*, $\tau_w/\tau_a = 0.156$; *4*, $\tau_w/\tau_a = 0.78$. Time is scaled according to Eq. 6.

given value of the ratio assures a unique system response in the central zone for the scaled concentration and the scaled time provided the aspect ratio, Eq. 3c, is large. The response for a particular case can be obtained by converting the scaled concentration and time to dimensioned quantities by means of the normalizing concentration, C^*, and the diffusion relaxation time, τ_a, given by Eq. 6.

Fig. 4 shows the approach to the steady state in the central zone in terms of the scaled time for a broad range of values of the time scale ratio τ_w/τ_a, Eq. 8. Although it is not convenient to relate these curves to real time, they are presented in this way because of their generality. The plot can be interpreted directly in real time for two cases. First, only the tubing wall diffusivity varies. Thus, increasing D_w decreases τ_w/τ_a and the time to steady state. Second, only the tube inner radius varies. Thus, increasing r_i decreases τ_w/τ_a and the time to steady state. Both conclusions are intuitively obvious. Other circumstances cannot be so easily interpreted.

The relation between the time (scaled to τ_a) required to reach 90% equilibration in the dialyzed zone and the time scale ratio, τ_w/τ_a, is approximately linear and given by

$$T_{0.9} = 0.8 + 57.6\,(\tau_w/\tau_a)$$
$$7.8 \times 10^{-3} \leq \tau_w/\tau_a \leq 7.8 \times 10^{-1}. \quad (9)$$

This general result is useful for predicting the time to steady state in any system. An analysis of the real time to steady state, predicted by Eq. 9, as a function of each of the geometric and material parameters of the system, shows that in all cases the real time function is comprised of two fairly flat plateaus joined by a very steep transition zone. Table IV presents one such analysis for illustration. The transition zone corresponds to the switch between the tubing wall and axoplasm as the rate-determining step in the approach to the steady state. The midpoint of the transition occurs at a value of τ_w/τ_a of ~0.05. Thus, for $\tau_w/\tau_a > 0.05$, the tubing wall determines equilibration rate while for $\tau_w/\tau_a < 0.05$, the axoplasm determines the rate. This condition is useful for predicting whether a change in dialysis tubing geometry (radius and wall thickness) is desirable, and whether changes in axon size will affect equilibration time significantly.

Knowledge of D_a and D_w is necessary before equilibration time can be estimated for most typical experimental conditions by means of Eqs. 8 and 9. The ratio of small solute diffusivities in axoplasm and free solution, D_a/D_t, is commonly in the range 1/2 to 1 except for strongly bound solutes such as Ca, where D_a/D_t could be 1/10 or 1/20 (Hodgkin and Keynes, 1957; Gilbert, 1975; Baker and Schapira, 1977). A dialysis tubing porosity of ~10%, D_w/D_t, is typical (Brinley and Mullins, 1967). Farrell and Babb (1973) measured D_w/D_t for organic solutes of 50 to 1,000 daltons in regenerated cellulose acetate membranes, and obtained the empirical correlation (derived from their Tables I and IV):

$$D_w = 33.12\,D_t^{1.502}. \quad (10)$$

Using Eq. 10, D_w/D_t ranges from 7 to 14% for free solution D_t in the range 5×10^{-6} to 2×10^{-5} cm^2/s. This range covers most solutes used experimentally. Table V presents 90% equilibration times predicted by means of Eqs. 8–10, and the condition that D_a/D_t is 1/2 or 1. It can be seen that for the most common solutes, equilibration times are relatively insensitive to axon size or to the actual D_a/D_t ratio. Most solutes should reach 90% equilibration within 15 min, while simple inorganic ions such as Na or K should equilibrate within 5 min. Strongly bound solutes like Ca, in the absence of a freely diffusable buffer such as EGTA, will require more equilibration time, and because $\tau_w/\tau_a <$ 0.05, the time will be very sensitive to axon size but insensitive to changes in tubing geometry or porosity. Assuming $D_w/D_t = 0.1$, $D_a = 5 \times 10^{-7}$ cm^2/s, and $D_t = 10^{-5}$ cm^2/s for Ca, the 90% equilibration time is 14 min in a 500 μm axon and 34 min in a 800 μm axon.

As noted in the theoretical discussion, the value of the similarity parameter *PER*, defined by Eq. 4d, which measures the relative contribution of the cell membrane solute flow to the axoplasmic concentration field, is extremely small for typical physiological and experimental conditions. However, it is of interest to define the contribution of the cell membrane permeability to system performance and to establish a level at which cell membrane flow affects the concentration field significantly. Such results can also be interpreted for the equivalent condition that the membrane flow is actually a chemical reaction at the cell membrane. Such results are useful for assessing the degree of control of substrates such as ATP, which is consumed by the Na, K pump. Fig. 5 presents the steady-state mean solute concentration at the cell membrane as a function of the cell permeability. The corresponding range for the similarity parameter *PER*, Eq. 4d, is 3.6×10^{-5} to 36. Control of the concentration is at least 95% complete, provided the permeability is $<3 \times 10^{-6}$ cm/s, or if *PER*

TABLE IV
REAL EQUILIBRATION TIMES

	τ_w/τ_a	=	0.008	0.016	0.078	0.156	0.781
(D_w constant)	$T_{0.9}$	=	810	551	343	318	297
(D_a constant)	$T_{0.9}$	=	81	110	343	635	2,968

Real times ($T_{0.9}$, s) required to reach 90% equilibration at the cell membrane for different values of D_a or D_w. Other parameters are the same as in Table II. τ_w/τ_a varied by changing only D_a or only D_w.

TABLE V
PREDICTED REAL EQUILIBRATION TIMES

r_a	D_a/D_t	$D_t \times 10^6$						
		1.5	3	5	7.5	10	15	20
250	1	85	30.4	14.9	7.9	5.2	2.9	1.9
250	1/2	87.8	31.9	15.2	8.5	5.7	3.2	2.1
400	1	91.8	33.8	16.4	9.2	6.2	3.6	2.3
400	1/2	101	38.7	19.3	11.2	7.7	4.5	3.0

Prediction of 90% solute equilibration times (min) for a range of seven free solution diffusivities ($D_t \times 10^6$, cm^2/s) and two axon sizes (r_a, μm). Dialysis tubing size given in Table II. Axoplasm/free solution diffusivity ratios, D_a/D_t, are either 1 or 1/2. Eqs. 8 and 9 were used.

<0.01. The permeability restriction applies only to the specific conditions of Table II, whereas the restriction on *PER* is general.

We can utilize Fig. 5 to estimate the effect of ATP consumption on the ATP concentration at the cell membrane, assuming all other ATP reactions are inhibited and 3 Na ions are pumped per ATP consumed. The active Na efflux is ~40 pmol/cm^2 s in squid axons when the nominal axoplasmic ATP concentration is ~4 mM (Brinley and Mullins, 1968). This corresponds to an apparent cell membrane permeability to ATP of 10^{-5} cm/s, and, according to Fig. 5, ATP at the cell membrane should be reduced by ~13% during dialysis. On the other hand, when axoplasmic ATP is 50 μM the efflux of Na through the pump is ~20 pmol/cm^2 s (Brinley and Mullins, 1968), corresponding to an apparent $P = 4 \times 10^{-4}$ cm/s for ATP. According to Fig. 5, ATP at the cell membrane will be reduced by 85% to a concentration of only 7.5 μM if 3 Na/ATP are transported at these low ATP levels. Dialysis control of ATP under these conditions would be very inadequate. Strategies such as used by Brinley and Mullins (1968) to provide an extra source of ATP by means of phosphoarginine are clearly essential for control of low levels of ATP by dialysis.

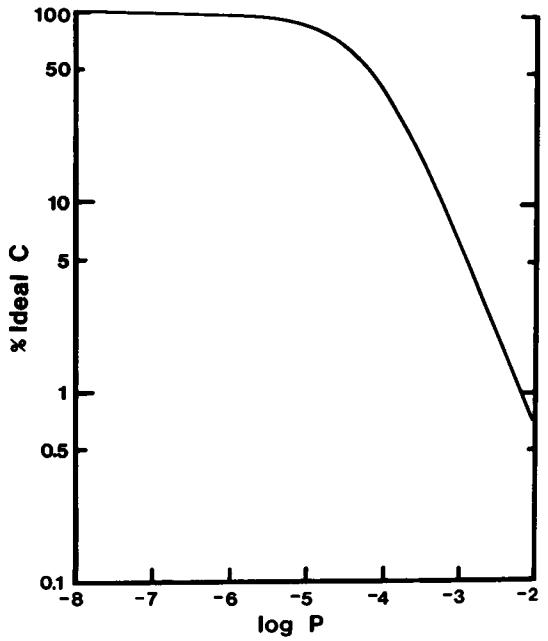

FIGURE 5 Effect of the cell membrane permeability (cm/s) to solute on the steady-state mean concentration at the cell membrane as percent of the ideal concentration with perfect equilibration. Log-log scales. Specific parameters used were those of Table II.

Influx Conditions. The initial conditions used for the preceding results are appropriate for the loading up or washing out of solute by means of dialysis. Influx conditions require that the initial solute concentration in axoplasm and the solute concentration in dialysis solution be zero. The time scale for influx is determined by the cell permeability, Eq. 7. The normalized extracellular solute concentration is taken to be 1 over some portion of the axon including the dialyzed zone, and is 0 over the remainder of the axon. This condition is established experimentally by appropriate guard procedures (Brinley et al., 1975; Dipolo, 1979). These procedures involve pumping the specific solute-containing solution past only the central dialyzed zone of the axon. Solute-free solution is pumped continually past the undialyzed axon ends. Under proper conditions, the two solutions do not mix significantly, and the interfaces between them define the boundaries for influx. Ideally, these boundaries are close to the ends of the dialyzed zone and are well defined. Poor control of these boundaries will cause over- or underexposure of the axon to solute relative to the dialyzed zone, resulting in possibly serious errors. It is important to estimate the magnitude of such errors.

Influx is estimated experimentally by measuring the appearance of a tracer solute in the dialysis solution effluent. End effects are a major concern in such work. Axial diffusion of solute between dialyzed and undialyzed zones of the axon might seriously alter the solute flow in dialyzate effluent relative to the true transmembrane solute flow over a well-defined section of the cell. Furthermore, if significant solute loading of the undialyzed axon ends occurs, followed by a large experimental reduction of the influx, axial diffusion of this excess solute into the central zone might seriously distort the new measured flux.

Numerical solutions were obtained, subject to the large aspect ratio restriction, for cell permeabilities in the range 10^{-8} to 10^{-2} cm/s. Confidence in the computer program was reinforced when it was found that the concentration field for influx (when subtracted from 1), when the entire external axon is exposed to solute, converged to that for efflux in the steady state over the entire range of permeabilities.

As noted in the discussion of similarity parameters the quantity *PER*, Eq. 4d, has some importance for influx. Because most normal resting membrane permeabilities are of order 10^{-6} cm/s or smaller, a $PER << 0.01$ is to be

expected. Based on the efflux results, this fact means that dialysis should control the solute concentration at the membrane fairly well, and that axoplasmic solute levels should be very low. The cell membrane itself is the rate-determining step in influx. Radial diffusion through the axon and tubing wall should not contribute much to end effects. The key factors in the end effect are axial diffusion in axoplasm and the rate of solute loading through the membrane as determined by the permeability.

The predictions about the important factors for influx were borne out when it was found that, for $PER < 0.01$, the scaled end effects are insensitive to the values of solute diffusivity and axon size within normal ranges (results not shown). Indeed, the end effects do not differ significantly for permeabilities of 10^{-8} to 10^{-6} cm/s, nor do results differ significantly for this same P range for the case of a step change of P during an experiment provided the (new/old) P ratio is constant. This latter point is a consequence of the fact that axial diffusion which contributes directly to the end effect occurs over a short distance and can adjust adequately to different solute loading rates. Because of these findings, results do not have to be given in terms of scaled time, and can be treated as sufficiently general to apply to most influx experiments using typical solutes and axons.

The end effect for influx is defined as the ratio of the total axial solute flow between the dialyzed and undialyzed axon regions to the total inflow of solute across the cell membrane in the dialyzed zone. This is essentially the error to be expected when influx is measured by monitoring solute levels in the dialyzate effluent. The quantitative results presented are not completely general because the membrane flow in the dialyzed zone depends on the absolute length of the dialyzed zone whereas the end effect is independent of this length when the aspect ratio is large. Since the dialyzed length is taken to be 1 cm in this work, end effect errors reported herein can be corrected to any other dialyzed length by simple division of the error by the actual length.

Fig. 6 presents results for several cases in which the amount of axon exposed to external solute differs from the dialyzed length. With the exception of complete exposure of the axon to external solute, the end effect develops very slowly and approaches an asymptote within 1 h. The influx error remains <5% provided external solute is not present more than 1 mm beyond each end of the dialyzed zone. The error increases rapidly when more than 1 mm of each undialyzed axon end is exposed to solute. When the solute exposure zone is only 0.4 mm less than the dialyzed zone the error is <1% at all times (not shown).

Solutes such as Ca, in the absence of a freely diffusable buffer like EGTA, have very small axoplasmic diffusivities. End effects for such solutes do not conform to Fig. 6. However, axial diffusion is so slow in this case that end effects are very small. Even for the case of complete

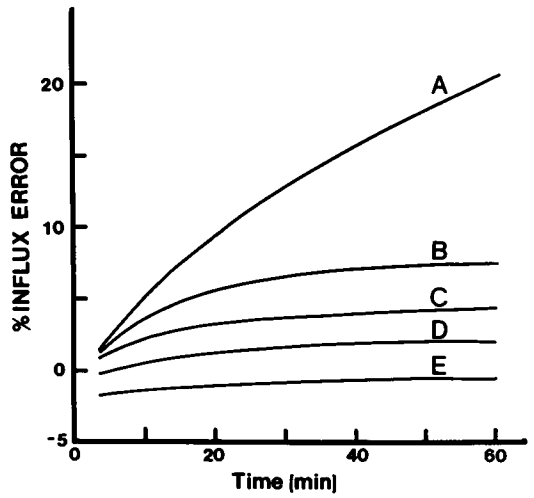

FIGURE 6 Development in time (min) of the influx error as percent of the true influx across the cell membrane in the central zone of the axon. A negative error means that significant axial diffusion from the central zone into the undialyzed axon ends occurs. Dialyzed zone width is 1 cm. Width of the zone of exposure to extracellular solute is *A*, 3 cm; *B*, 1.34 cm; *C*, 1.2 cm; *D*, 1.1 cm; and *E*, 1.0 cm. Error is <1% at all times for an exposure of 0.92 cm,and is not shown for reasons of legibility.

exposure of the axon to external solute, the end effect is <10% after 3 h (results not shown) when $D_a = 5 \times 10^{-7}$ cm^2/s. Fig. 6 applies for $D_a \geq 5 \times 10^{-6}$ cm^2/s, or values appropriate to most common solutes used in dialysis work.

Fig. 7 shows the end effects in response to a 10-fold reduction of influx following 25 min of influx at the higher

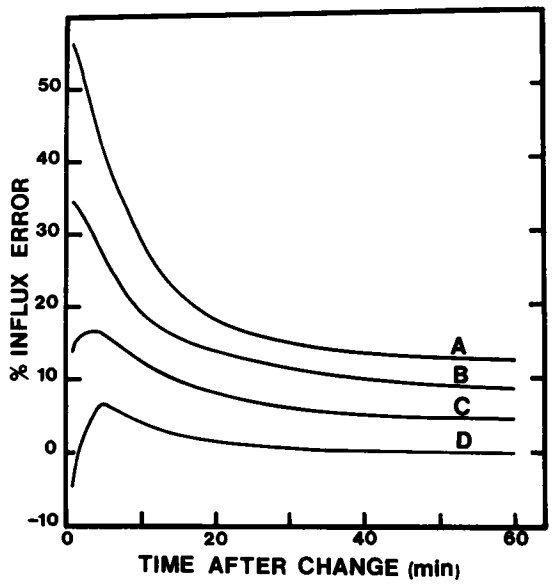

FIGURE 7 Development in time (min) of the influx error as percent of the true influx across the cell membrane in the central zone of the axon following a 10-fold reduction of the cell membrane permeability. Dialysis at the higher permeability proceeded for 25 min prior to the change. Dialyzed zone width is 1 cm. Width of zone of exposure to extracellular solute is *A*, 1.34 cm; *B*, 1.2 cm; *C*, 1.1 cm; and *D*, 1.0 cm. Error is <1% at all times for an exposure of 0.92 cm and is not shown for reasons of legibility.

rate. The end effect is more sensitive to the amount of axon exposed to external solute in this case. When the exposure is 1 mm beyond the dialyzed ends, 40 min is required for the error to fall below 10%. Even greater axon exposure would result in large errors throughout a typical experiment. When the solute exposure zone is only 0.4 mm less than the dialyzed zone, the error is <1% at all times (not shown). If influx at the higher rate proceeds for 50 min before the flux reduction, the end effects do not differ significantly from those at 25 min (not shown). A quasi-steady state in solute concentration near the dialyzed boundary is established. Of course once the far axon ends fill up with solute by axial diffusion, after many hours, the end effects must increase.

A 100-fold decrease of the influx will produce much larger end effect errors (not shown). If the exposure to external solute is coincident with the dialyzed zone, ~45 min is required for the error to fall below 10%. However, when the exposure zone is only 0.4 mm less than the dialyzed zone, the error is < 2% at all times.

It is clear that if the external solute exposure zone is slightly less than the dialyzed zone, end effects can be ignored, and for most conditions if exposure overlaps the dialyzed zone by no more than 1 mm on each end, the end effects will not cause serious errors. This requires, however, that great care be taken to control the exposure zone, such as by the methods of Dipolo (1979) or Brinley et al. (1975). A common experimental test for end effects is to observe the washout of solute from the axon when extracellular solute is removed. Fig. 8 presents the tails of washout curves calculated for four solute exposure zones. Analytically these tails are distinct, but practically a modest excess external solute exposure of only 1 mm beyond each dialyzed end may not be distinguishable from ideal exposure. This fact is especially relevant when the experimental protocol involves very large changes of the influx. An alternative measure for the importance of end effects is the time to steady state following a sudden large reduction of the influx. This could be effected by changing the membrane potential, or the extracellular solute concentration, or by the application of external rapid-acting inhibitors. The approach to a new steady-state flux estimate would parallel the tails of the error curves of Fig. 7. The time required to come within 90% of the final steady state increases monotonically with the amount of excess external solute exposure. This time would be <10 min for excess exposures of <1 mm each end, ~10 min for 1 mm excess each end, and ~15 min for a 1.7 mm excess each end. This test also is not very sensitive because the time resolution or the solute detection efficiency of the experiments may not be adequate.

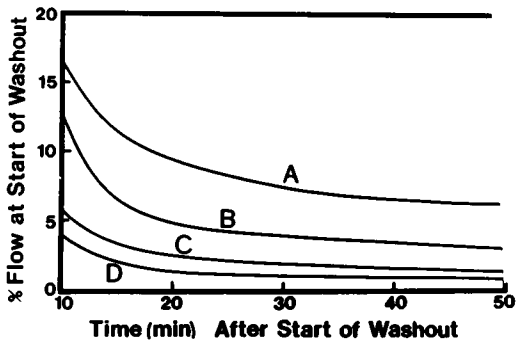

FIGURE 8 Washout of solute from axon upon termination of an influx experiment. Solute flow in dialysis solution effluent as percent of the flow prior to removal of extracellular solute is plotted against the time elapsed from the start of washout (min). First 10 min of washout is not plotted because curves are complicated, tending to cross each other. Width of dialyzed zone 1 cm. Width of zone of exposure to extracellular solute is *A*, 3.0 cm; *B*, 1.34 cm; *C*, 1.1 cm; and *D*, 1.0 cm. Tail of curve for exposure of 0.92 cm is very similar to *D*, and is not shown for reasons of legibility.

It is concluded that end effects for strongly bound solutes such as Ca, in the absence of a freely diffusable buffer, would be small for long time periods when P is constant, even if the entire axon is exposed to external solute. This is borne out further by the solute washout test where, for complete exposure of the axon to external solute, the washout tail is <5% of the steady solute flow in dialyzate within 25 min of the removal of external solute (results not shown), whereas for the same conditions with K ion, more than an hour is required to reach the same level. Thus, for solutes in which $\tau_w/\tau_a < 0.05$ end effect errors are likely to be small even when end guarding is poor.

The time to steady state in a well-guarded axon during an influx experiment can be longer or shorter than the time for the corresponding efflux experiment. In this case, the conditions approximate pure radial diffusion in a composite medium. Reference to the analytic solution of the case of a uniform cylinder wall (Crank, 1956, p. 79) shows that even in this simpler case influx and efflux are not symmetric. This is a consequence of the geometric effect of curvature on the structure of the solute concentration fields. In fact, for the dialysis problem the time to steady state during well-guarded influx depends strongly on similarity parameters given by Eqs. 4b–d. No simple correlations were found, but in no case did the equilibration time exceed the corresponding efflux time by more than 50%, and in most cases the influx time was very similar to or slightly less than the corresponding efflux time.

Finite Flow of Dialyzate

Efflux Conditions. The approach of the central-dialyzed zone to a steady state and the development of end effects should be slower at finite dialyzate flow rate. It is useful to have some idea of the time required to establish a steady state at finite flow, and to estimate the uniformity of the concentration field at the membrane in the steady state. Because calculations of finite flow are extremely difficult (up to 5 h computer time) it was not feasible to address these questions completely. However, results are

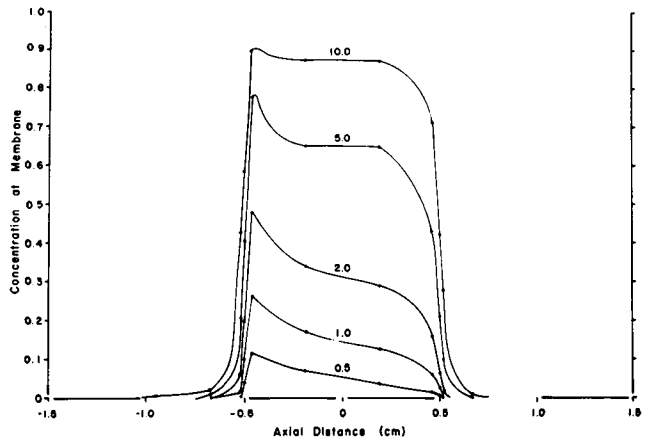

FIGURE 9 Development of axial solute concentration field at the cell membrane in 500 μm axon dialyzed over 1 cm at a finite dialysis solution flow of 0.44 μl/min. Cf. Fig. 2 for further explanation.

presented below for solute loading or unloading by dialysis and the parameter group given in Table II.

Fig. 9 shows the development of the concentration field at the cell membrane though 10 radial diffusion time scales for the case of a low dialyzate flow rate and a 1-cm dialysis zone. At 17 times scales, the mean concentration is within 95% of ideal. It is clear that dialysis is effective at this flow rate and ultimately should establish a concentration field at the membrane similar to that at infinite flow rate. A dialyzate flow rate of 2.2 μl/min with a 6-mm dialysis zone gives an equilibration curve very similar to the infinite flow rate curve. At a dialyzate flow rate of 0.22 μl/min with a 6-mm dialysis zone a steady-state membrane flow equal to that established by infinite dialyzate flow rate should be reached in ~30 time scales. This corresponds to ~30 min of real time, and is certainly a practical experimental limit. The time to steady state for finite dialyzate flow rate depends not only on the τ_w/τ_a ratio, Eq. 8, but also on the mean transit time of dialyzate through the dialysis zone:

$$\overline{T} = 4\, l_t/U. \tag{11}$$

Within the range of $\overline{T}$ tested, it is still true that the dialysis membrane is rate-determining when $\tau_w/\tau_a > 0.05$. At most practical flow rates, the real time to steady state is insensitive to the axoplasm diffusivity or axon size, provided $\tau_w/\tau_a > 0.05$. The restriction should apply to most solutes except those that may be strongly bound, such as Ca. This means that a mixture of many solutes can be controlled by dialysis at finite flow rate, and an overall steady state established, roughly simultaneously. However, for bound solutes, having small τ_w/τ_a ratios, the time to steady state can be twofold or more longer than the time for freely diffusible solutes. Furthermore, improvement of the tubing porosity, D_w/D_t, cannot be expected to increase the equilibration rate for bound solutes because the cytoplasm is rate-determining anyway.

The practical question of concern for finite flow rates is how sensitive the equilibration rate is to the dialyzate flow rate or, more properly, to the axial mean transit time of fluid through the lumen of the permeable zone of tubing. One might expect that if radial diffusion is very slow in axoplasm or in the tubing wall then the equilibration time will be fairly insensitive to dialyzate flow rate because, in one mean transit time, so little solute can leave the dialysis solution that its concentration is not reduced much. Therefore, the system response will not deviate significantly from the infinite flow case. At the other extreme, if diffusion is very fast relative to the dialyzate flow rate, the system will behave like a perfectly mixed tank, and the equilibration time will depend more strongly on $\overline{T}$. When conditions are not extreme, the equilibration rate will be sensitive to the radial concentration gradients that exist at any time. The structure of the radial concentration field should depend not only on how rapidly solute is supplied by dialyzate flow but also on relative diffusion rates expressed as radial diffusion time scales in the dialysis solution, wall, and axoplasm.

Numerical solutions were obtained for different τ_w/τ_a and $\overline{T}$. D_w and D_t were unchanged and equal to the values given in Table II. $\overline{T}$ was varied either by changing the dialyzate flow rate at constant l_t or by changing l_t subject to the aspect ratio restriction. The range of flow rates used was 0.22 to 2.2 μl/min, similar to those used experimentally. The corresponding mean transit times ranged from 1.2 to 11.6 s. Results are independent of absolute magnitudes of parameters, provided the following similarity conditions are not changed: Eq. 8 for τ_w/τ_a and

$$\tau_t/\tau_w = (D_w/D_t)[r_i/(r_o - r_i)]^2$$

and

$$\overline{T}/\tau_t = (D_t/r_i^2)\,(4l_t/U). \tag{12}$$

The time (scaled to τ_a) required to reach 90% equilibration is approximately a linear function of the scaled mean transit time. The slope of the relation depends on τ_w/τ_a. The relation is

$$T_{0.9} = T^{\infty}_{0.9}\,[1 + B\,(\overline{T}/\tau_t)] \tag{13}$$

where $T^{\infty}_{0.9}$ is the corresponding time for infinite flow conditions and can be estimated by Eq. 9, and $\overline{T}/\tau_t$ is given by Eq. 12. Note that Eq. 13 also gives the real time if $T^{\infty}_{0.9}$ is converted to real time. The slope B was determined for three values of τ_w/τ_a:

τ_w/τ_a	B
0.008	0.09
0.08	0.32
0.16	0.25.

We see that for small τ_w/τ_a the equilibration time is relatively insensitive to dialysis solution flow rate, as predicted. Maximal flow sensitivity occurs at an intermediate value of τ_w/τ_a, probably near 0.05. At large τ_w/τ_a,

flow sensitivity is still fairly high but significantly less than maximal.

The relationship for equilibration time, Eq. 13, has considerable utility for experimental design and for evaluating experimental results involving transitions between steady states. Assuming the empirical correlation of Farrell and Babb (1973) applies via Eq. 10, expected real equilibration times for various solute diffusivities can be calculated by means of Eqs. 8–13. Such calculations show that for small D_t the percent change in equilibration time relative to infinite dialysis flow is small. While the percent change for large D_t is large, the real time at infinite flow is so small that the time increase at finite flow is not of practical importance. For example, the time changes from 1.9 min at infinite flow to 6.3 min at 0.4 μl/min when $D_t = 2 \times 10^{-5}$ cm^2/s, given the parameters of Table II. For the common D_t range of 5×10^{-6} to 2×10^{-5} cm^2/s and a typical experimental dialysis solution flow of 2 μl/min most solutes used experimentally should reach 90% equilibration within 20 min, even in an 800 μm axon,and solutes such as Na, K, or Cl should equilibrate within 5 or 10 min. Practically, a mixture of common solutes will equilibrate almost simultaneously at any dialysis flow. Finite dialysis flows, in the range used experimentally, should not retard equilibration times to any practical extent.

DISCUSSION

Calculations confirm the qualitative assessment of the effectiveness of internal dialysis derived from extensive use of the method. Predicted control of solute concentration at the cell membrane is better than 99.9% of ideal over the dialyzed zone when the cell membrane is impermeable to solute. When P is of the order of 10^{-7} cm/s, predicted control is at least 99% of ideal, while it is at least 98% of ideal when P is 10^{-6} cm/s. The presence of undialyzed axon ends does not affect control significantly, provided the aspect ratio is >10. The numerical procedures are not sufficiently accurate to resolve uncertainties about extreme situations where it is desired to establish a concentration of <1/1,000 the initial value in order to minimize a rate process of very high affinity for the solute. ATP is the most likely candidate for such extremes, but because it is essentially impermeable to the cell membrane, a 1,000-fold reduction of its concentration at the cell membrane over 90% of the dialyzed zone can be expected, provided no axoplasmic production occurs.

Effects due to undialyzed axon ends can be significant during influx experiments unless good end-guarding procedures are used. End effects can be ignored if the dialyzed zone is slightly wider (by ~0.5 mm) than the zone of exposure to the extracellular tracer solute. If the extracellular exposure zone is ~1 mm wider than the dialysis zone, end effects are small unless very large reductions of influx occur. Care in controlling the exposure zone for external tracer solute is important when the experiment involves large influx reductions. The presence of poor end-guarding might be detected by observing the time to steady state following a step change of influx, or the washout of tracer solute at the end of an experiment. However, these checks are sufficiently sensitive only if solute detection efficiency and time resolution are very good. The most conservative approach to minimizing end effects is to make the dialysis zone ~1 mm wider than the external solute exposure zone. Then precise end-guarding is not essential. Error in the influx estimates would be due primarily to uncertainty about the true length of the exposure zone, and this can be easily kept to <10% if the apparent zone is longer than 1 cm.

The relationships derived for prediction of the 90% equilibration time for infinite and finite dialysis flows are only approximate but should provide estimates within 20% of the true theoretical times. Although valid only for efflux conditions, they should give reasonable order of magnitude estimates for the corresponding influx experiments that will be nearly as good as efflux estimates in most cases. The relations are useful for the design of experimental protocols including choice of axon size (where possible) or dialysis tubing size and wall thickness, tubing porosity (where possible), dialysis flow rate, proper length of the dialyzed zone, and prediction of the time periods required to establish steady states following experimental manipulations of the flux or cell membrane. Time predictions can be used to evaluate the adequacy of dialysis in actual experiments.

Finally, control of axoplasm composition is effective even at very low dialysis solution flows if sufficient time is provided. About 30 min or less would be required to reach a steady state with most solutes at a flow of 0.2 μl/min. Although this time would be unacceptable in experiments requiring numerous steady-state transitions it is not exceptionally long. The fact that such low flows can establish a good steady state means that it is not necessary to maintain the high dialysis flows usually used throughout an experiment. Expensive isotopes can be conserved by reducing the dialysis flow once the steady state is reached. Higher flows are required only during transitions between steady states.

Supported by National Institutes of Health grants NS 14569 and NS 18868, and special research funds from the University of Maryland Computer Science Center and the Temple University Computer Activity Center.

Received for publication 21 October 1981 and in final form 27 January 1983.

REFERENCES

Abramowitz, M., and I. A. Stegun, editors. 1964. Handbook of Mathematical Functions. NBS Applied Mathematics Series. Vol. 55. U. S. Government Printing Office, Washington, D.C. 771–802.

Baker, P., and A. Schapira. 1977. Measurement of ionic diffusion and

mobility in axoplasm isolated from giant axons of *Myxicola*. *J. Physiol.* (*Lond.*). 266:5P.

Brinley, F. J., and L. Mullins. 1967. Sodium extrusion by internally dialyzed squid axons. *J. Gen. Physiol.* 50:2303–2331.

Brinley, F. J., and L. Mullins. 1968. Sodium fluxes in internally dialyzed squid axons. *J. Gen. Physiol.* 52:181–211.

Brinley, F. J., S. G. Spangler, and L. J. Mullins. 1975. Calcium and EDTA fluxes in dialyzed squid axons. *J. Gen. Physiol.* 66:223–250.

Carslaw, H. S., and J. C. Jaeger. 1959. Conduction of Heat in Solids. Oxford University Press, London.

Crank, J. 1956. The Mathematics of Diffusion. Oxford University Press, London.

Dipolo, R. 1979. Calcium influx in internally dialyzed squid giant axons. *J. Gen. Physiol.* 73:91–113.

Farrell, P., and A. Babb. 1973. Estimation of the permeability of cellulosic membranes from solute dimensions and diffusivities. *J. Biomed. Mater. Res.* 7:275–300.

Gear, C. W. 1971. Numerical Initial Value Problems in Ordinary Differential Equations. Prentice-Hall, Inc., Englewood Cliffs, NJ.

Gilbert, D. 1975. Axoplasm architecture and physical properties as seen in the *Myxicola* giant axon. *J. Physiol.* (*Lond.*). 253:257–301.

Hodgkin, A. L., and R. D. Keynes. 1957. Movements of labelled calcium in squid giant axons. *J. Physiol.* (*Lond.*). 138:253–281.

Lanczos, C. 1956. Applied Analysis. Prentice-Hall, Inc., Englewood Cliffs, NJ.

Villadsen, J., and J. Sorensen. 1969. Solution of parabolic partial differential equations by a double collocation method. *Chem. Eng. Sci.* 24:1337–1349.

Villadsen, J., and W. Stewart. 1967. Solution of boundary value problems by orthogonal collocation. *Chem. Eng. Sci.* 22:1483–1501.